

SCIENTIFIC REPORTS



OPEN

Antisense oligonucleotide and thyroid hormone conjugates for obesity treatment

Yang Cao¹, Tomoko Matsubara^{2,3}, Can Zhao^{1,4}, Wei Gao^{1,5}, Linxiu Peng⁶, Jinjun Shan⁶, Zhengxia Liu^{1,4}, Fang Yuan^{1,7}, Lingyi Tang^{1,7}, Peixin Li^{2,8}, Zhibin Guan⁹, Zhuyuan Fang⁷, Xiang Lu⁵, Hu Huang² & Qin Yang¹

Using the principle of antibody-drug conjugates that deliver highly potent cytotoxic agents to cancer cells for cancer therapy, we here report the synthesis of antisense-oligonucleotides (ASO) and thyroid hormone T3 conjugates for obesity treatment. ASOs primarily target fat and liver with poor penetrance to other organs. Pharmacological T3 treatment increases energy expenditure and causes weight loss, but is contraindicated for obesity treatment due to systemic effects on multiple organs. We hypothesize that ASO-T3 conjugates may knock down target genes and enrich T3 action in fat and liver. Two established ASOs are tested. Nicotinamide N-methyltransferase (NNMT)-ASO prevents diet-induced obesity in mice. Apolipoprotein B (ApoB)-ASO is an FDA approved drug for treating familial hypercholesterolemia. NNMT-ASO and ApoB-ASO are chemically conjugated with T3 using a non-cleavable sulfo-SMCC linker. Both NNMT-ASO-T3 (NAT3) and ApoB-ASO-T3 (AAT3) enhance thyroid hormone receptor activity. Treating obese mice with NAT3 or AAT3 decreases adiposity and increases lean mass. ASO-T3 enhances white fat browning, decreases genes for fatty acid synthesis in liver, and shows limited effects on T3 target genes in heart and muscle. Furthermore, AAT3 augments LDL cholesterol-lowering effects of ApoB-ASO. Therefore, ASO and hormone/drug conjugation may provide a novel strategy for obesity and hyperlipidemia treatment.

The antibody-drug conjugates (ADCs) or immunoconjugates have emerged as a novel class of drugs for targeted cancer therapy^{1,2}. ADC is a three-component system in which a therapeutic monoclonal antibody (mAb) and a potent small-molecule cytotoxic drug are conjugated through a stable linker. The mAb specifically recognizes the surface antigen/receptor on cancer cells, which blocks signal transduction. At the meantime, the ADC complex is internalized into cancer cells, where the antibody is degraded and the cytotoxic drug is released. This unique design not only significantly decreases the side effects of cytotoxic drugs, but also allows enrichment of cytotoxic drugs in cancer cells³. Two ADC drugs brentuximab vedotin and ado-trastuzumab emtansine have been approved by FDA for the treatment of lymphoma and breast cancer¹. Many ADC drugs are currently on clinical trials for cancer therapy⁴.

Intrigued by the ADC design, we asked whether a similar strategy could be used for obesity treatment by targeting metabolic organs. Since there are no established antibodies suitable for the ADC design, we turned our focus to antisense oligonucleotides (ASO) as a potential replacement for antibodies. ASOs are modified short single-chain DNA molecules that regulate gene expression primarily in liver and fat⁵⁻⁷. The ASOs have very

¹Department of Medicine, Physiology and Biophysics, UC Irvine Diabetes Center, Center for Epigenetics and Metabolism, University of California Irvine, Irvine, California, 92697, USA. ²Department of Kinesiology & Physiology, East Carolina Diabetes and Obesity Institute, East Carolina University, Greenville, North Carolina 27834, USA. ³Japan Society for the Promotion of Science, Tokyo, 1020083, Japan. ⁴Department of Geriatrics, the Second Affiliated Hospital, Nanjing Medical University, Nanjing, 211166, China. ⁵Department of Geriatrics, Sir Run Run Shaw Hospital, Nanjing Medical University, Nanjing, 211166, China. ⁶Medical Metabolomics Center, Jiangsu Key Laboratory of Pediatric Respiratory Disease, Nanjing University of Chinese Medicine, Nanjing, 210023, China. ⁷Department of Cardiology, the First Affiliated Hospital of Nanjing University of Chinese Medicine, Nanjing, 210029, China. ⁸Department of Comprehensive Surgery, Medical and Health Center, Beijing Friendship Hospital, Capital Medical University, Beijing, China. ⁹Department of Chemistry, University of California, Irvine, 92697, California, USA. Yang Cao and Tomoko Matsubara contributed equally to this work. Correspondence and requests for materials should be addressed to H.H. (email: huangh@ecu.edu) or Q.Y. (email: qin.yang@uci.edu)

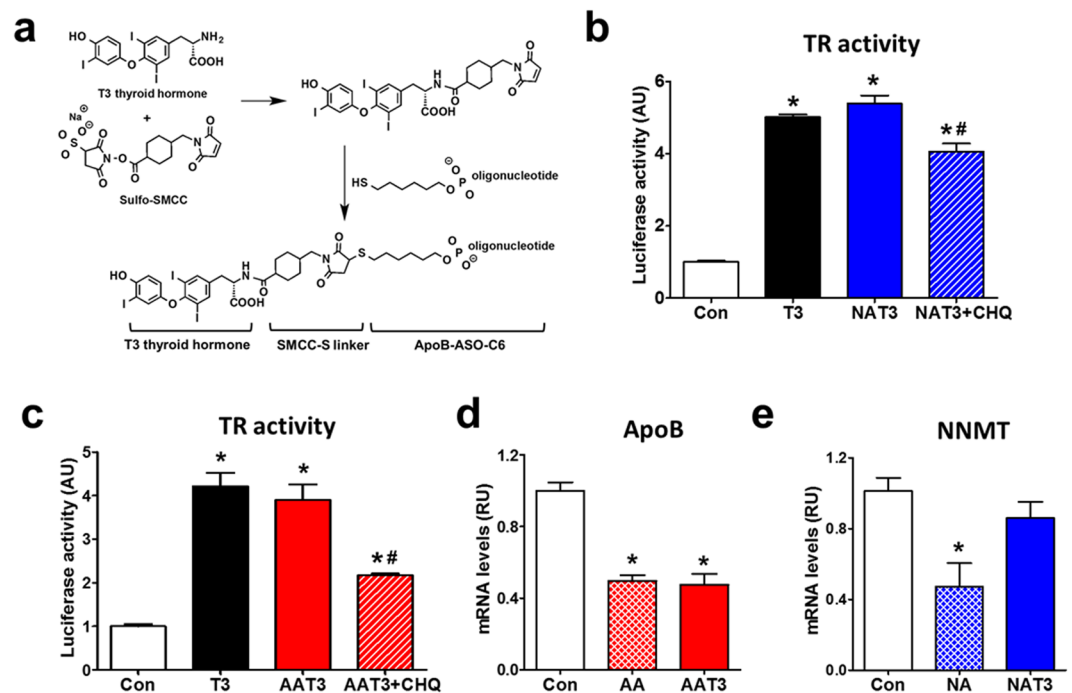


Figure 1. ASO-T3 conjugate structure and function. **(a)** Schematic process of ASO-T3 synthesis. **(b–c)** Thyroid hormone receptor reporter activity in HEK293 cells treated with T3, NNMT-ASO-T3 (NAT3) **(b)** or ApoB-ASO-T3 **(c)** with or without the lysosome inhibitor chloroquine (CHQ). **(d)** ApoB mRNA levels in Hepa1-6 hepatoma cells treated with ApoB-ASO (AA) or AAT3. **(e)** NNMT mRNA levels in adipose tissue treated NNMT-ASO (NA) or NAT3. $n = 4–6$ per group; * $p < 0.05$ vs controls (Con), # $p < 0.05$ vs NAT3 or AAT3.

poor bioavailability in skeletal and cardiac muscle, brain, pancreas, following systemic administration^{6–8}. In fact, significant efforts have been made towards designing ASO modifications to improve the penetrance to organs other than liver and fat⁹. This limitation of ASOs to treat neurological, muscular and cardiac diseases turns to be advantageous to design ASO-drug conjugates to target fat and liver for obesity treatment. Another important consideration for choosing ASOs is that, similar to cellular uptake of ADC, ASO internalization is shown to be largely through endocytosis^{10,11}.

Increasing energy expenditure is a major strategy for obesity treatment. Thyroid hormone T3 is very powerful in increasing basal metabolic rate and inducing browning of white adipose tissue^{12,13}. Weight loss is a major symptom of hyperthyroidism in humans¹⁴. However, thyroid hormone is contraindicated for obesity treatment due to its systemic effects on brain, heart and muscle causing anxiety, heart failure, and muscle wasting¹⁴. Since ASOs penetrate these organs very poorly, we hypothesize that ASO-T3 conjugates would minimize the thyroid hormone effects in these organs.

The next question is what linker to use to conjugate ASOs and T3. We chose sulfosuccinimidyl-4-(*N*-maleimidomethyl)cyclohexane-1-carboxylate (Sulfo-SMCC), a non-cleavable and membrane impermeable crosslinker, because of its high selectivity, rapid reaction kinetics, and compatibility with aqueous reaction conditions¹⁵. Sulfo-SMCC contains an amine-reactive *N*-hydroxysuccinimide (NHS ester) and a sulfhydryl-reactive maleimide group. The maleimide group of Sulfo-SMCC is unusually stable because of the cyclohexane bridge in the spacer arm. This significantly increases ADC drug stability in circulation. Sulfo-SMCC has been widely used in the synthesis of ADCs including FDA-approved ado-trastuzumab emtansine.

We then tested two established ASOs. Nicotinamide *N*-methyltransferase (NNMT) is a histone methylation modulator that regulates cellular energy expenditure in adipose tissue^{16,17}. NNMT-ASO treatment prevents diet-induced obesity¹⁶. The FDA-approved drug Mipomersen is an ASO against Apolipoprotein B (ApoB) for treating familial hypercholesterolemia⁵. Using the concept of ADC design, we synthesized novel compounds by chemically conjugating NNMT-ASO and ApoB-ASO with T3 hormone using sulfo-SMCC linker. We then investigated the effects of the ASO-T3 bioconjugates on obesity.

Results

ASO-T3 synthesis and function. Thyroid hormone T3 was first reacted with sulfo-SMCC to generate maleimide-activated T3. The product was then conjugated to phosphorothioate-modified NNMT-ASO or ApoB-ASO (Fig. 1a). The NNMT-ASO-T3 (NAT3) and ApoB-ASO-T3 (AAT3) products show no detectable free T3 or T3-SMCC (Supplementary Figure 1a–d). The successful conjugation of ASO and T3 was verified by MALDI-TOF MS (Supplementary Figure 2a,b). We then investigated whether ASO-T3 conjugates may maintain the functionality of both ASO and T3. NAT3 and AAT3 activated thyroid hormone receptor reporter (Fig. 1b,c). The effects were attenuated by the treatment of chloroquine, an inhibitor of lysosome acidification, suggesting that lysosome

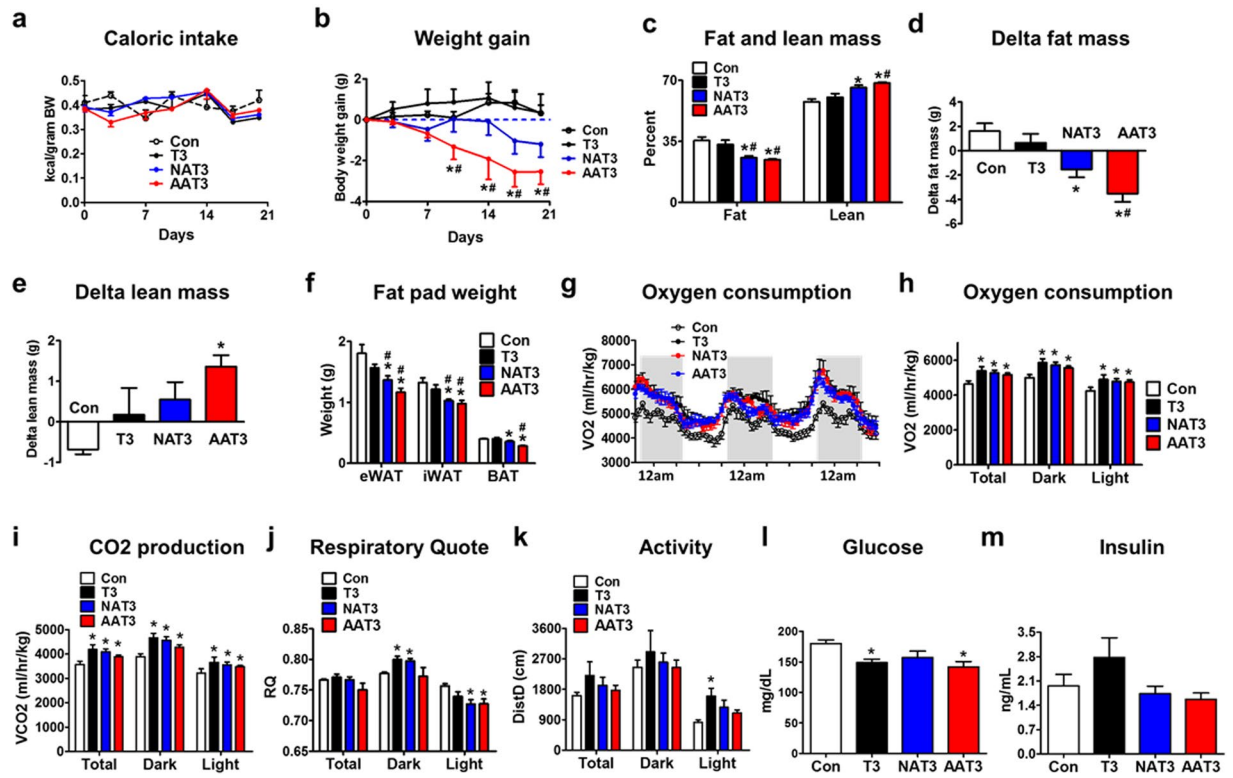


Figure 2. ASO-T3 reduces adiposity in obesity. (a–f) Caloric intake (a), body weight gain (b), percent fat and lean mass (c), delta fat mass (d), delta lean mass (e) and weight of epididymal (eWAT), inguinal (iWAT) and brown (BAT) adipose tissue (f) in high-fat diet fed mice treated with PBS control, T3, NNMT-ASO-T3 (NAT3) or ApoB-ASO-T3 (AAT3). (g–k) Metabolic cages studies. Oxygen consumption (g,h) and CO₂ production (i) normalized to lean mass, respiratory quote (j) and locomotor activity (k) in control, T3, NAT3 and AAT3-treated mice. (l) Glucose; (m) insulin levels in control, T3, NAT3 and AAT3-treated mice. n = 4–6 per group; *p < 0.05 vs controls (Con), #p < 0.05 vs T3.

plays an important role in T3 activity of NAT3 and AAT3 (Fig. 1b,c). The ASO activity in ASO-T3 conjugates appears to be target-dependent. AAT3 decreased ApoB expression to the similar degree as ApoB-ASO (AA) in cultured hepatocytes (Fig. 1d), while NAT3 failed to knock down NNMT expression in cultured hepatocytes, adipocytes (not shown) or adipose tissue (Fig. 1e). Since NAT3 has no NNMT-ASO activity and ApoB-ASO is known to have no effects on body weight in animals and humans^{18,19}, we focused on studying the effects of AAT3 and NAT3 on energy expenditure and weight loss.

Effects of ASO-T3 on obesity. T3 treatment increased serum T3 by approximately 8 times, while NAT3 and AAT3 did not significantly alter circulating T3 levels (Supplementary Fig. 3a). Interestingly, T3 treatment did not decrease, but increased body weight in mice fed a high fat diet (Supplementary Fig. 3b), despite significantly elevated energy expenditure (Supplementary Fig. 3c). The increased food intake^{20,21} (Supplementary Fig. 3d) and enhanced nutrient absorption²² may contribute to the weight gain in T3-treated mice. We therefore performed pair-feeding experiments. Caloric intake was not different in mice treated with control, T3, NAT3 or AAT3 (Fig. 2a). Despite pair-feeding, T3 treatment did not decrease body weight in three weeks. NAT3 treatment resulted in mild weight loss and AAT3 was a more potent ASO-T3 bioconjugate to induce weight loss (Fig. 2b). NAT3 and AAT3, but not T3 decreased fat mass and increased lean mass (Fig. 2c–e). Consistently, individual depot mass including epididymal fat, inguinal fat and brown fat were all decreased in NAT3 and AAT3-treated mice compared to control and T3-treated mice (Fig. 2f). In the metabolic cage studies, T3, NAT3 and AAT3 all elevated oxygen consumption and CO₂ production (Fig. 2g–i). NAT3 and AAT3 decreased respiratory ratio compared to control and T3 treatment during light cycles, indicating increased fat metabolism (Fig. 2j). T3 also significantly increased locomotor activity during the light cycles compared with controls (Fig. 2k), which might be due to anxiety and/or food-seeking behavior. Glucose levels were lower in T3, NAT3 and AAT3-treated mice (Fig. 2l). Insulin levels tended to be higher with T3 treatment, but lower in NAT3 and AAT3 treated mice (Fig. 2m). These results indicate that ASO-T3 conjugates are effective in increasing energy expenditure and treating obesity in mice.

Effects of ASO-T3 treatment on T3 target gene expression in metabolic organs. Treatment of T3, NAT3 and AAT3 all induced the expression of browning markers in inguinal white adipose tissue (iWAT) (Fig. 3a,b). NAT3 and AAT3 were stronger in inducing Ucp1 expression comparing with T3 (Fig. 3a). It is

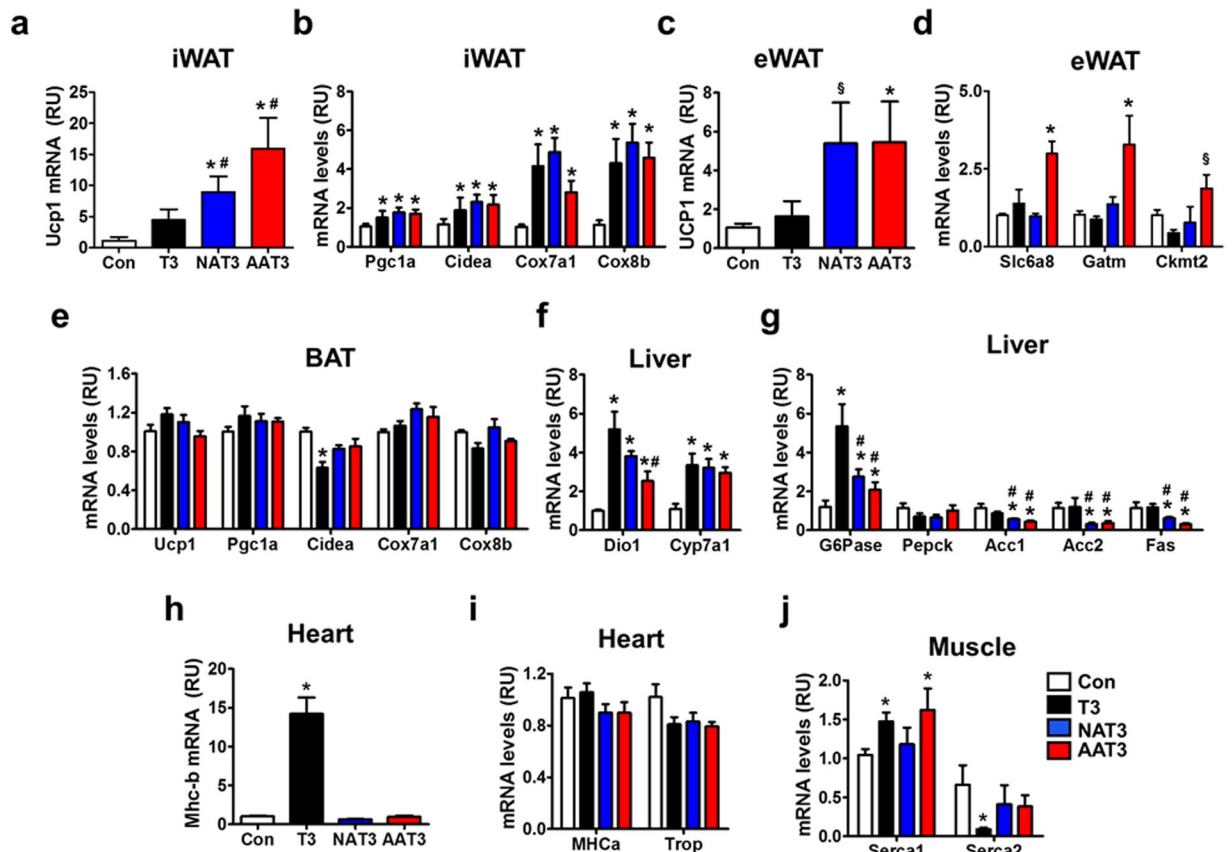


Figure 3. Effects of ASO-T3 on gene expression in metabolic organs. (a,b) Browning markers (Ucp1, Pgc1a, Cidea, Cox7a1 and Cox8b) in inguinal white adipose tissue (iWAT). (c) Ucp1 expression in epididymal white adipose tissue (eWAT). (d) Expression of solute carrier family 6 member 8 (Slc6a8), glycine amidinotransferase (Gatm) and creatine kinase mitochondrial 2 (Ckmt2) in eWAT. (e) Expression of brown adipose tissue (BAT) gene markers. (f) Hepatic expression of thyroid hormone responsive genes deiodinase-1 (Dio1) and cholesterol 7 α -hydroxylase (Cyp7a1). (g) Gluconeogenic genes (G6pase, Pepck) and fatty acid synthesis genes (Acc1, Acc2 and Fas) in liver. (h,i) Expression of Mhc-b (h) and Mhc-a and Troponin (Trop) (i) in heart. (j) Expression of Serca1 and Serca2a in muscle. NAT3: NNMT-ASO-T3; AAT3: ApoB-ASO-T3. n = 4–6 per group; *p < 0.05 vs control, #p = 0.07 vs control, \$p < 0.05 vs T3.

recently reported that epididymal white adipose tissue (eWAT) may also participate in thermogenic response via Ucp1-dependent and creatine dependent pathways²³. Interestingly, NAT3 and AAT3 both elevated Ucp1 expression in eWAT (Fig. 3c). In addition, AAT3 increased expression of Slc6a8, Gatm and Ckmt2, the genes involved in creatine metabolism (Fig. 3d). These results suggest that thermogenic activation in eWAT may also contribute to the increased energy expenditure in ASO-T3-treated mice. In brown adipose tissue (BAT), neither T3, NAT3 nor AAT3 had significant effects on BAT activity (Fig. 3e). In liver, NAT3 and AAT3 appeared to have comparable or lower activity on the thyroid hormone target genes such as Dio1, Cyp7a1 and G6pase, compared with T3 alone (Fig. 3f,g). However, NAT3 and AAT3 had stronger effects on suppressing fatty acid synthesis as evidenced by decreased expression of Acc1, Acc2 and Fas compared with control and T3 treatment (Fig. 3g). In heart, T3 treatment drastically increased the expression of Mhc-b, a marker for cardiac failure, by approximately 13 times compared with controls. NAT3 and AAT3 did not affect Mhc-b expression (Fig. 3h). Neither T3, NAT3 nor AAT3 affected the expression of Mhc-a or troponin (Fig. 3i). In skeleton muscle, thyroid hormone differentially regulates the isoforms of the Ca²⁺-ATPase (Serca) by increasing the fast-muscle isoform (Serca1) and suppressing the slow-muscle isoform (Serca2)²⁴. Consistently, we found that T3, but not NAT3 increased Serca1. For unknown reasons, AAT3 also increased Serca1 expression. T3 strongly suppressed Serca2a expression while NAT3 and AAT3 had no effects (Fig. 3j). These results indicate that ASO-T3 selectively regulates thyroid hormone target genes in adipose tissue and liver.

ApoB-ASO and T3 conjugates improve hypercholesterolemia. AAT3 maintained the ASO activity in cultured hepatocytes (Fig. 1d). In mice treated with AAT3, the ApoB expression was slightly lower than that in AA-treated mice (Fig. 4a). The serum LDL levels was significantly decreased in AAT3-treated mice compared that in AA-treated mice (Fig. 4b). The results suggest potential synergistic effects of AA and T3 on lowering LDL levels in obesity.

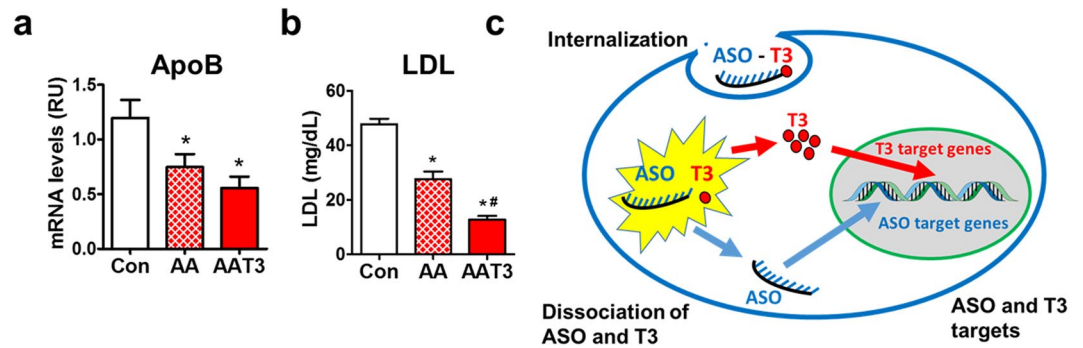


Figure 4. Effects of ApoB-ASO-T3 (AAT3) on LDL levels. (a) Apolipoprotein B (ApoB) mRNA levels in liver. (b) Serum LDL levels. AA: ApoB-ASO. $n = 5-6$ per group; * $p < 0.05$ vs controls, ** $p < 0.05$ vs AA. (c) Schematic working model for ASO-T3 action. ASO-T3 is internalized and processed in cells. ASO knocks down the target gene and T3 exerts its biological functions by activating nuclear thyroid hormone receptor.

Discussion

Despite our better understanding of the pathophysiology of obesity, the drug development for obesity treatment is lagging behind. Increasing energy expenditure to overcome energy intake is a fundamental strategy for obesity drug development²⁵. Many drugs such as thyroid hormone and adrenergic receptor agonists are quite potent in increasing energy expenditure²⁶⁻²⁸. However, the systemic effects of these drugs prohibit the use for obesity treatment. The situation is similar to the cytotoxic drugs for cancer therapy. Although effective in killing cancer cells, cytotoxic drugs also significantly damage normal tissues. The art of ADC drug design brings a therapeutic revolution in cancer treatment, allowing targeted delivery of cytotoxic drugs to cancer cells. Using the concept of ADC design and taking advantages of adipose and hepatic targeting effects of ASOs, we successfully developed ASO-T3 conjugates. Recently, a hybrid hormone of glucagon-T3 conjugation has been reported to selectively target adipose tissue and liver leading to remarkable weight loss and improvement of metabolic syndrome in obese mice²⁹. Therefore, the novel drug design to induce adipose and hepatic hyperthyroidism may lead to a new direction for drug development for the treatment of obesity and metabolic syndrome.

The ideal outcome of ASO-T3 design is to retain both ASO and T3 activity so that ASO can knock down the target gene and T3 can activate thyroid hormone receptors in fat and liver. The goal is to achieve synergistic effects of ASO and T3 on improving glucose, lipid and energy metabolism. However, conjugation of small molecules to ASOs may affect ASO stability and activity^{29, 30}. For the two ASO-T3 conjugates we tested, only ApoB-ASO-T3 maintains the ASO activity, while NNMT-ASO-T3 fails to knock down NNMT. Therefore, careful ASO selection and testing are critical to successful ASO-T3 conjugation.

Although both T3 and ASO-T3 increase energy expenditure, only ASO-T3 treated mice show reduced body weight and adiposity. Different from weight loss in hyperthyroid humans, euthyroid mice treated with T3 systemically do not lose, but gain weight. This is largely due to the direct effects of T3 on hypothalamus to stimulate food intake and effects on intestine to increase nutrient absorption in mice²⁰⁻²². Despite pair feeding, energy expenditure and absorption appear to be balanced in T3-treated mice. In ASO-T3-treated mice, however, circulating T3 is not elevated. Thus, there is no systemic T3 action to compensate the increased energy expenditure, leading to weight loss and reduced adiposity.

One important consideration to use ASOs as the tissue-homing vector is that ASOs, similar to the antibodies in ADC, are internalized into tissue cells by endocytosis *in vivo*^{10, 11} (Fig. 4c). The physiological endocytosis process does not damage the integrity of cellular plasma membrane and therefore less toxic. Intracellularly, ASOs are either degraded in lysosomes directly or hybridized with RNAs and degraded by nucleases^{10, 31, 32}. Inhibition of lysosome acidification with chloroquine decreased, but did not completely abolish T3 activity (Fig. 1b,c), suggesting that both pathways might be involved in the ASO and T3 dissociation in cultured cells.

Although effective in treating obesity, the current ASO-T3 drug design could be further improved to increase the T3 payload and delivery efficiency. In the ADC design, many chemotherapy drug molecules are conjugated to the cysteine or lysine residues at different positions of one antibody molecule, which maximizes cytotoxic effects³. Since ASOs are much smaller molecules compared with antibodies, one ASO is conjugated to one T3 molecule. Whether adding multiple T3 to one ASO molecule is feasible remains to be tested. In addition, the activity of ASO-T3 on thyroid hormone receptor reporter is about 1/1000 compared with that of T3 in our *in vitro* assays (Fig. 1b,c). Approaches such as testing different conjugation linkers³³ may increase the dissociation between ASO and T3 to enhance the biological activity of both ASO and T3. Finally, although liver is the primary target organ for ASOs, the preference of ASO accumulation in liver is the non-parenchymal cells rather than hepatocytes³⁴⁻³⁶. This may at least partially explain the relatively lower expression of Dio1, a very sensitive marker for hepatic thyroid hormone activity³⁷, in ASO-T3 treated mice compared with that in T3-treated mice. Future studies to add modifications such as triantennary N-acetyl galactosamine³⁴⁻³⁶ or adipose-targeting peptide^{38, 39} to ASOs may increase the bioavailability of ASO-T3 in liver and adipose tissue. Despite these limitations, the current drug design provides a prototype model for a new class of drugs for treating obesity.

In summary, using the principle of ADC, we have successfully designed ASO-T3 conjugates and proved the concept that ASO-T3 may represent a novel strategy for drug development for obesity treatment. Importantly, ApoB-ASO (Mipomersen) is an FDA-approved drug with established safety profiles for treating familial hypercholesterolemia. ApoB-ASO-T3 conjugate may potentially be used for general obese patients with hypercholesterolemia.

Materials and Methods

ASO-T3 synthesis. Phosphorothioate-modified ASOs^{16,19} (mouse NNMT-ASO: 5-GAAATGAACCAGCAG GCCTT-3 and mouse ApoB-ASO: 5-GTCCCTGAAGATGTCAATGC-3) with a 5'- thiol and C6 amino linker were synthesized by Bio-Synthesis (Lewisville, Texas). Thyroid hormone T3 was first reacted with sulfo-SMCC to generate maleimide-activated T3. After reversed-phase high-performance liquid chromatography (RP-HPLC) purification, excessive T3-SMCC is reacted with the thiol-functionalized oligonucleotides to generate ASO-T3 conjugates. The conjugates were purified by RP-HPLC and characterized by MALDI-TOF MS.

Thyroid hormone receptor activity. HEK293T cells were maintained in Dulbecco's modified Eagle's medium supplemented with L-glutamine, 10% steroid hormone-depleted fetal calf serum, penicillin and streptomycin. Transient transfections were performed in 6-well plates of subconfluent cells. Two-step transfections were performed because no luciferase activity could be measured when the plasmids were co-transfected with ASOs (not shown). Plasmids including thyroid hormone receptor alpha (100 ng), thyroid hormone receptor beta (100 ng), DR4-luciferase thyroid hormone receptor (100 ng) and PRL-TK (10 ng) were first transfected to HEK293T cells using FuGENE HD transfection reagent (Roche)⁴⁰. Twelve hours later, ASO-T3 (1 μ M) was transfected to the cells. Luciferase activity was measured 36 hours after the ASO-T3 transfection. The DR4-driven Firefly luciferase activity was normalized to PRL-TK-driven Renilla luciferase activity. Chloroquine (100 μ M) was added to inhibit lysosome acidification 6 hours prior to luciferase activity measurements. T3 (1 nM) was added 24 hours prior to cell harvesting for positive controls of thyroid hormone reporter activity.

ASO-T3 treatment in mice. Wild type C57BL/6 mice were purchased from the Jackson Laboratory and housed in a 12-hour light/dark cycle (lights on 7 am-7 pm). The mice were first treated with a high fat diet (Research Diets D12331, 5.56 kcal/gm) for 12 weeks. An MRI was performed for the baseline body composition. The mice were then treated with PBS control, T3 (200 μ g/kg) or ASO-T3 (25 mg/kg) twice a week. The metabolic cage studies were started from day 7 when there was no difference in body weight. A repeat MRI was performed three weeks after the treatment. Mouse studies were conducted in accordance with federal guidelines and were approved by the Institutional Animal Care and Use Committee of University of California Irvine and East Carolina University.

Serum T3 measurements. Serum T3 was measured using liquid chromatography-tandem mass spectrometry (LC-MS/MS)^{41,42}. Eighty-microliter serum from mice treated with T3 or ASO-T3 for two hours was mixed with ascorbic acid, citric acid and dithiothreitol (25 μ g/ μ l) to prevent the potential conversions of thyroid hormones. After one-hour incubation on ice, 640 μ l urea was added and the solution was incubated at 50 °C for one hour. The samples were then subjected to solid phase extraction before the injection to the LC-MS/MS. Separation was achieved using GP-Phenyl (3 μ m, 2.1 \times 100 mm). The gradient mobile phase consisted of 0.1% formic acid in water (A) and acetonitrile (B) and the flow rate was set at 0.2 mL/min. Mass spectrometry detection was operated on TSQ Vantage Triple-Stage Quadrupole Mass Spectrometer, Spray voltage:3.2 KV, Vaporizer temperature:200 °C, Sheath gas pressure:45 arb, Aux gas pressure:15 arb, Capillary temperature:270 °C. The quantification was performed by the selected reaction monitoring (SRM) in the positive ionization mode and the parameters is m/z 651.517 \rightarrow 508.000 for T3 (CE of 22 eV; S-lens at 161 V), 461.095 \rightarrow 285.056 for IS (CE of 19 eV; S-lens at 88 V).

Body composition. Body composition was analyzed in mice treated with control PBS, T3, NNMT-ASO-T3 or ApoB-ASO-T3 for 3 weeks using an EchoMRI 3-in-1 instrument (Echo Medical Systems, Houston, TX).

Metabolic cages. Energy expenditure was evaluated using TSE PhenoMaster System. HFD-fed mice were treated with Control PBS, T3, NNMT-ASO-T3 or ApoB-ASO-T3 for 7 days. The mice were acclimated in the metabolic cages for 2 days before the experiments. CO₂ production and O₂ consumption were collected every 60 min for each mouse during a period of 3–4 days. The levels were normalized to the lean mass. Food intake and activity were measured at regular intervals.

Serum glucose, insulin and LDL measurements. Glucose levels were measured using the glucose colorimetry assay (Cayman Chemicals). Insulin was measured with Ultrasensitive Insulin ELISA kit (Crystal Chem). LDL was measured using LDL Assay kit from BioAssay Systems.

RNA extraction and quantitative PCR. Adipose tissue and liver RNA was extracted using RNeasy Mini Kit (Qiagen). RNA from heart and muscle was extracted using RNeasy Fibrous Tissue Mini kit (Qiagen). Hepa1-6 mouse hepatoma cells were transfected with ASO and ASO-T3. RNA was extracted 48 hours after transfection. SYBR Realtime PCR were performed as described previously⁴³. The primers are listed in Supplementary Table-1.

Statistical test. All data are expressed as mean \pm s.e.m. Analyses of variance were performed followed by Bonferroni-Holm posthoc tests for multiple comparisons. Statistical significance is assumed for $p < 0.05$.

References

1. Leal, M. *et al.* Antibody-drug conjugates: an emerging modality for the treatment of cancer. *Ann N Y Acad Sci* **1321**, 41–54 (2014).
2. Zolot, R. S., Basu, S. & Million, R. P. Antibody-drug conjugates. *Nat Rev Drug Discov* **12**, 259–260 (2013).
3. Weiner, G. J. Building better monoclonal antibody-based therapeutics. *Nat Rev Cancer* **15**, 361–370 (2015).
4. Bouchard, H., Viskov, C. & Garcia-Echeverria, C. Antibody-drug conjugates—a new wave of cancer drugs. *Bioorg Med Chem Lett* **24**, 5357–5363 (2014).
5. Crooke, S. T. & Geary, R. S. Clinical pharmacological properties of mipomersen (Kynamro), a second generation antisense inhibitor of apolipoprotein B. *Br J Clin Pharmacol* **76**, 269–276 (2013).

6. Popov, V. B. *et al.* Second-generation antisense oligonucleotides against beta-catenin protect mice against diet-induced hepatic steatosis and hepatic and peripheral insulin resistance. *FASEB J* **30**, 1207–1217 (2016).
7. Watts, L. M. *et al.* Reduction of hepatic and adipose tissue glucocorticoid receptor expression with antisense oligonucleotides improves hyperglycemia and hyperlipidemia in diabetic rodents without causing systemic glucocorticoid antagonism. *Diabetes* **54**, 1846–1853 (2005).
8. Zinker, B. A. *et al.* PTP1B antisense oligonucleotide lowers PTP1B protein, normalizes blood glucose, and improves insulin sensitivity in diabetic mice. *Proc Natl Acad Sci USA* **99**, 11357–11362 (2002).
9. Khvorova, A. & Watts, J. K. The chemical evolution of oligonucleotide therapies of clinical utility. *Nat Biotechnol* **35**, 238–248 (2017).
10. Koller, E. *et al.* Mechanisms of single-stranded phosphorothioate modified antisense oligonucleotide accumulation in hepatocytes. *Nucleic Acids Res* **39**, 4795–4807 (2011).
11. Marcusson, E. G., Bhat, B., Manoharan, M., Bennett, C. F. & Dean, N. M. Phosphorothioate oligodeoxyribonucleotides dissociate from cationic lipids before entering the nucleus. *Nucleic Acids Res* **26**, 2016–2023 (1998).
12. Mullur, R., Liu, Y. Y. & Brent, G. A. Thyroid hormone regulation of metabolism. *Physiol Rev* **94**, 355–382 (2014).
13. Obregon, M. J. Adipose tissues and thyroid hormones. *Front Physiol* **5**, 479 (2014).
14. Brent, G. A. Clinical practice. *Graves' disease*. *N Engl J Med* **358**, 2594–2605 (2008).
15. Hermanson, G. T. *Bioconjugate techniques*, (Academic Press, Amsterdam Netherlands; Boston Mass., 2008).
16. Kraus, D. *et al.* Nicotinamide N-methyltransferase knockdown protects against diet-induced obesity. *Nature* **508**, 258–262 (2014).
17. Ulanovskaya, O. A., Zuhl, A. M. & Cravatt, B. F. NNMT promotes epigenetic remodeling in cancer by creating a metabolic methylation sink. *Nat Chem Biol* **9**, 300–306 (2013).
18. Lee, R. G. *et al.* Comparison of the pharmacological profiles of murine antisense oligonucleotides targeting apolipoprotein B and microsomal triglyceride transfer protein. *J Lipid Res* **54**, 602–614 (2013).
19. Mullick, A. E. *et al.* Antisense oligonucleotide reduction of apoB ameliorated atherosclerosis in LDL receptor-deficient mice. *J Lipid Res* **52**, 885–896 (2011).
20. Hernandez, A. *et al.* Type 3 deiodinase deficiency results in functional abnormalities at multiple levels of the thyroid axis. *Endocrinology* **148**, 5680–5687 (2007).
21. Kong, W. M. *et al.* Triiodothyronine stimulates food intake via the hypothalamic ventromedial nucleus independent of changes in energy expenditure. *Endocrinology* **145**, 5252–5258 (2004).
22. Muller, M. J. & Seitz, H. J. Thyroid hormone action on intermediary metabolism. *Part I: respiration, thermogenesis and carbohydrate metabolism*. *Klin Wochenschr* **62**, 11–18 (1984).
23. Bertholet, A. M. *et al.* Mitochondrial Patch Clamp of Beige Adipocytes Reveals UCP1-Positive and UCP1-Negative Cells Both Exhibiting Futile Creatine Cycling. *Cell Metab* **25**, 811–822 e814 (2017).
24. Simonides, W. S., Thelen, M. H., van der Linden, C. G., Muller, A. & van Harveldt, C. Mechanism of thyroid-hormone regulated expression of the SERCA genes in skeletal muscle: implications for thermogenesis. *Biosci Rep* **21**, 139–154 (2001).
25. Hill, J. O., Wyatt, H. R. & Peters, J. C. Energy balance and obesity. *Circulation* **126**, 126–132 (2012).
26. Inokuma, K. *et al.* Indispensable role of mitochondrial UCP1 for antiobesity effect of beta3-adrenergic stimulation. *Am J Physiol Endocrinol Metab* **290**, E1014–1021 (2006).
27. Moore, R., Grant, A. M., Howard, A. N. & Mills, I. H. Treatment of obesity with triiodothyronine and a very-low-calorie liquid formula diet. *Lancet* **1**, 223–226 (1980).
28. Vosselman, M. J. *et al.* Systemic beta-adrenergic stimulation of thermogenesis is not accompanied by brown adipose tissue activity in humans. *Diabetes* **61**, 3106–3113 (2012).
29. Finan, B. *et al.* Chemical Hybridization of Glucagon and Thyroid Hormone Optimizes Therapeutic Impact for Metabolic Disease. *Cell* **167**, 843–857 e814 (2016).
30. Winkler, J., Saadat, K., Diaz-Gavilan, M., Urban, E. & Noe, C. R. Oligonucleotide-polyamine conjugates: influence of length and position of 2'-attached polyamines on duplex stability and antisense effect. *Eur J Med Chem* **44**, 670–677 (2009).
31. Crooke, S. T., Wang, S., Vickers, T. A., Shen, W. & Liang, X. H. Cellular uptake and trafficking of antisense oligonucleotides. *Nat Biotechnol* **35**, 230–237 (2017).
32. Juliano, R. L., Carver, K., Cao, C. & Ming, X. Receptors, endocytosis, and trafficking: the biological basis of targeted delivery of antisense and siRNA oligonucleotides. *J Drug Target* **21**, 27–43 (2013).
33. Lu, J., Jiang, F., Lu, A. & Zhang, G. Linkers Having a Crucial Role in Antibody-Drug Conjugates. *Int J Mol Sci* **17**, 561 (2016).
34. Graham, M. J. *et al.* *In vivo* distribution and metabolism of a phosphorothioate oligonucleotide within rat liver after intravenous administration. *J Pharmacol Exp Ther* **286**, 447–458 (1998).
35. Prakash, T. P. *et al.* Targeted delivery of antisense oligonucleotides to hepatocytes using triantennary N-acetyl galactosamine improves potency 10-fold in mice. *Nucleic Acids Res* **42**, 8796–8807 (2014).
36. Yu, R. Z. *et al.* Disposition and Pharmacology of a GalNac3-conjugated ASO Targeting Human Lipoprotein (a) in Mice. *Mol Ther Nucleic Acids* **5**, e317 (2016).
37. Maia, A. L., Kieffer, J. D., Harney, J. W. & Larsen, P. R. Effect of 3,5,3'-Triiodothyronine (T3) administration on *dio1* gene expression and T3 metabolism in normal and type 1 deiodinase-deficient mice. *Endocrinology* **136**, 4842–4849 (1995).
38. Azhdarinia, A. *et al.* A peptide probe for targeted brown adipose tissue imaging. *Nat Commun* **4**, 2472 (2013).
39. Kolonin, M. G., Saha, P. K., Chan, L., Pasqualini, R. & Arap, W. Reversal of obesity by targeted ablation of adipose tissue. *Nat Med* **10**, 625–632 (2004).
40. Makowski, A., Brzostek, S., Cohen, R. N. & Hollenberg, A. N. Determination of nuclear receptor corepressor interactions with the thyroid hormone receptor. *Mol Endocrinol* **17**, 273–286 (2003).
41. Hansen, M., Luong, X., Sedlak, D. L., Helbing, C. C. & Hayes, T. Quantification of 11 thyroid hormones and associated metabolites in blood using isotope-dilution liquid chromatography tandem mass spectrometry. *Anal Bioanal Chem* **408**, 5429–5442 (2016).
42. Wang, D. & Stapleton, H. M. Analysis of thyroid hormones in serum by liquid chromatography-tandem mass spectrometry. *Anal Bioanal Chem* **397**, 1831–1839 (2010).
43. Gao, W. *et al.* Retinol-binding protein 4 induces cardiomyocyte hypertrophy by activating TLR4/MyD88 pathway. *Endocrinology*, en20152022 (2016).

Acknowledgements

The study was supported by grants from the NIH (R01 DK100385) to Q.Y.; East Carolina University Start-up fund to H.H.; the National Science Foundation of China (No. 81270428 and No. 81470501) to X.L.; the National Natural Science Foundation of China (No. 81273713 and No. 81573909) to Z.F.; the Postgraduate Research and Innovation Project in Jiangsu Province, China (JX22013318) and the China Scholarship Council (1410150039) to W.G.; scholarship from the China Scholarship Council (201608320234) to C.Z.

Author Contributions

Q.Y. and H.H. conceived the project, analyzed data and wrote the manuscript. Y.C., T.M., C.Z., W.G., L.P., J.S., Z.L., F.Y., L.T., P.L. performed the experiments. Z.G. helped with ASO-T3 design. Z.F., X.L. contributed to the

project discussion. All authors reviewed and approved the manuscript. Q.Y. is the guarantor of this work and, as such, had full access to all the data in the study and takes responsibility for the integrity of the data and the accuracy of the data analysis.

Additional Information

Supplementary information accompanies this paper at doi:[10.1038/s41598-017-09598-z](https://doi.org/10.1038/s41598-017-09598-z)

Competing Interests: Q.Y. is an inventor on a patent application related to NNMT.

Publisher's note: Springer Nature remains neutral with regard to jurisdictional claims in published maps and institutional affiliations.



Open Access This article is licensed under a Creative Commons Attribution 4.0 International License, which permits use, sharing, adaptation, distribution and reproduction in any medium or format, as long as you give appropriate credit to the original author(s) and the source, provide a link to the Creative Commons license, and indicate if changes were made. The images or other third party material in this article are included in the article's Creative Commons license, unless indicated otherwise in a credit line to the material. If material is not included in the article's Creative Commons license and your intended use is not permitted by statutory regulation or exceeds the permitted use, you will need to obtain permission directly from the copyright holder. To view a copy of this license, visit <http://creativecommons.org/licenses/by/4.0/>.

© The Author(s) 2017